

## Effects of inertia in forced corner flows

By C. HANCOCK†, E. LEWIS

School of Mathematics, University of Bristol

AND H. K. MOFFATT

Department of Applied Mathematics and Theoretical Physics,  
University of Cambridge

(Received 24 October 1980 and in revised form 12 June 1981)

When viscous fluid is contained in the corner between two planes intersecting at an angle  $\alpha$ , a flow may be 'forced' either by relative motion of the two planes keeping  $\alpha$  constant (the 'paint-scraper' problem – Taylor 1960) or by relative rotation of the planes about their line of intersection (the hinged-plate problem – Moffatt 1964). In either case, a similarity solution is available describing the flow sufficiently near the corner, where inertia forces are negligible. In this paper, we investigate the effects of inertia forces, by constructing regular perturbation series for the stream function, of which the leading term is the known similarity solution. The first-order inertial effect is obtained analytically, and, for the Taylor problem with  $\alpha = \frac{1}{2}\pi$ , 25 terms of the perturbation series for the wall stress are generated numerically. Analysis of the coefficients suggests that the radius of convergence of the series is given by  $r|U|/\nu \approx 9.1$ , where  $r$  is distance from the corner,  $U$  is the relative speed of the planes, and  $\nu$  is the kinematic viscosity of the fluid. For the hinged-plate problem, discussed in § 5, the unsteadiness of the flow contributes to an inertial effect which is explicitly incorporated in the analysis. For both problems, streamline plots are presented which indicate the first influence of inertia forces at distances from the corner at which these become significant.

---

### 1. The corner problem of Taylor (1960)

When incompressible viscous fluid is contained in the corner between two planes  $\theta = 0, \alpha$  (figure 1), and when one of the planes ( $\theta = 0$ ) is moved parallel to itself with steady velocity  $U$ , the flow that is generated is dominated by viscous forces sufficiently near to the corner. In this region, the stream function  $\psi_s(r, \theta)$ , which satisfies the biharmonic equation, is given by the similarity solution (Taylor 1960, 1962)

$$\psi_s = rUf_1(\theta) = rU(B \sin \theta + C\theta \cos \theta + D\theta \sin \theta), \quad (1.1)$$

where

$$B = \frac{-\alpha^2}{\alpha^2 - \sin^2 \alpha}, \quad C = \frac{\sin^2 \alpha}{\alpha^2 - \sin^2 \alpha}, \quad D = \frac{\alpha - \sin \alpha \cos \alpha}{\alpha^2 - \sin^2 \alpha}. \quad (1.2)$$

The streamlines  $\psi_s = \text{constant}$  are shown (for  $\alpha = \frac{1}{2}\pi$ ) by the solid curves of figure 1; the flow is, in this approximation, reversible, so that, if  $U$  is replaced by  $-U$ , the arrows on the streamlines are reversed, but the streamline pattern is unaffected.

† Present address: Bath College of Higher Education, Newton Park, Bath BA2 9BN.

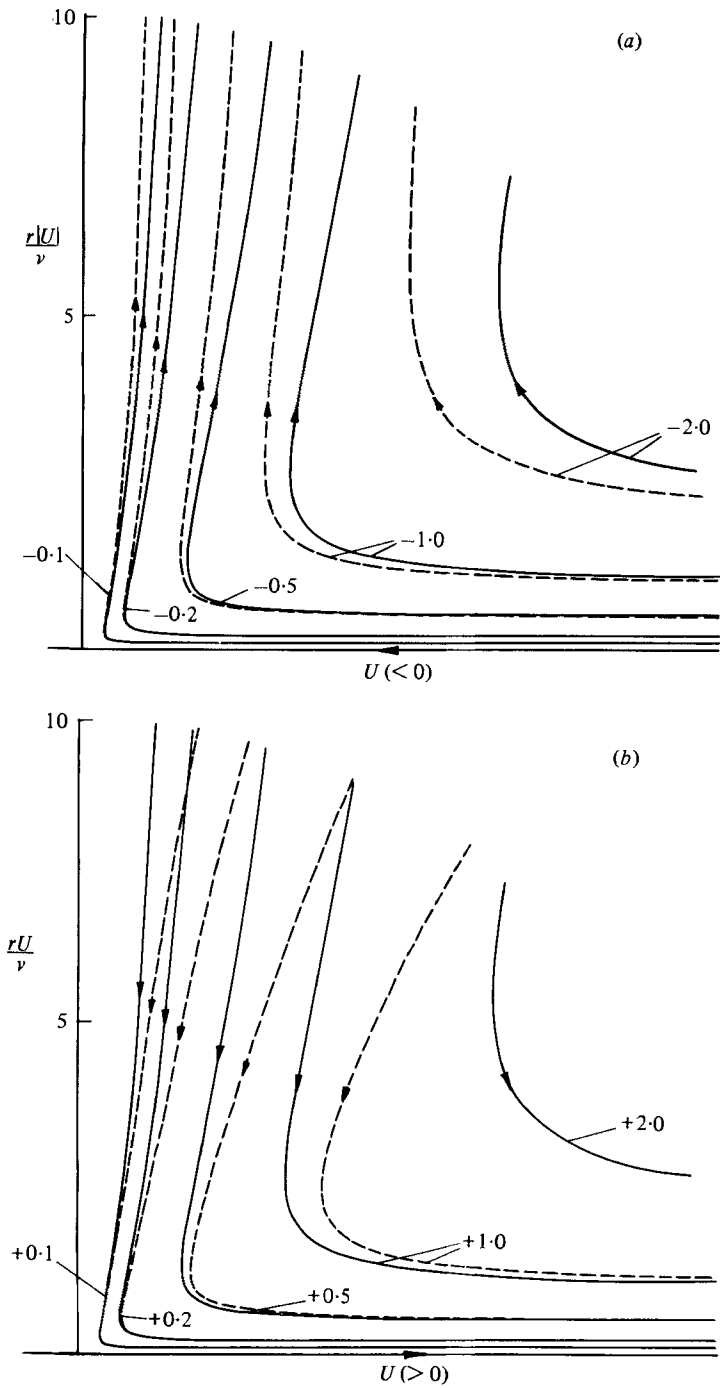


FIGURE 1. Streamlines for the Taylor corner problem with  $\alpha = \frac{1}{2}\pi$ ; the solid curves are the streamlines of the Stokes flow  $\psi_1 (= \psi_s/\nu) = \text{constant}$ ; the dashed lines are the streamlines  $\psi_1 + \psi_2 = \text{constant}$ , including the first inertial correction (obtained analytically).

The above solution breaks down at a distance of order  $\nu/|U|$  from the origin (where  $\nu$  is the kinematic viscosity of the fluid) due to the increasing importance of inertia as  $r$  increases. † In order to analyse inertial effects, we consider the exact equation for the stream function  $\psi(r, \theta)$ , viz

$$\nu \nabla^4 \psi = -\frac{1}{r} \frac{\partial(\psi, \nabla^2 \psi)}{\partial(r, \theta)}, \tag{1.3}$$

and we seek to solve this, subject to the boundary conditions

$$\left. \begin{aligned} \psi &= 0, & \partial\psi/\partial\theta &= -rU & \text{on } \theta &= 0, \\ \psi &= 0, & \partial\psi/\partial\theta &= 0 & \text{on } \theta &= \alpha. \end{aligned} \right\} \tag{1.4}$$

We may anticipate the asymptotic behaviour

$$\psi \sim \psi_s(r, \theta) \quad \text{as } r \rightarrow 0. \tag{1.5}$$

The natural procedure is simply to seek the solution in the form of a regular perturbation expansion ‡

$$\psi = \nu \sum_1^\infty \psi_n(r, \theta), \quad \text{where } \psi_n = \left(\frac{rU}{\nu}\right)^n f_n(\theta), \tag{1.6}$$

with  $f_1(\theta)$  given by (1.1). Substitution in (1.3) yields a sequence of equations

$$\nabla^4 \psi_n = -\frac{1}{r} \sum_{i+j=n} \frac{\partial(\psi_i, \nabla^2 \psi_j)}{\partial(r, \theta)} \quad (n = 2, 3, \dots), \tag{1.7}$$

and this in turn yields a sequence of linear inhomogeneous equations for the  $f_n(\theta)$ , viz

$$\left(\frac{d^2}{d\theta^2} + n^2\right) \left(\frac{d^2}{d\theta^2} + (n-2)^2\right) f_n = -\sum_{i+j=n} \left( i f_i \frac{d}{d\theta} - (j-2) f_i' \right) \left(\frac{d^2}{d\theta^2} + j^2\right) f_j \tag{1.8}$$

( $n = 2, 3, \dots$ ).

Since  $\nu\psi_1$  already satisfies the boundary conditions (1.4), equations (1.8) are to be solved subject to the homogeneous boundary conditions

$$f_n = f_n' = 0 \quad \text{on } \theta = 0, \alpha \quad (n = 2, 3, \dots). \tag{1.9}$$

## 2. Possible ‘eigenfunction’ contributions

Before carrying out this procedure, there is a possible complication that needs comment. At the lowest order in the expansion (1.6), the solution  $\psi_s = \nu\psi_1$  is not unique (regarded as a solution of the biharmonic equation satisfying the boundary conditions (1.4)) but may be supplemented by the general solution  $\psi_c(r, \theta)$  of the homogeneous problem

$$\nabla^4 \psi_c = 0, \quad \psi_c = \partial\psi_c/\partial\theta = 0 \quad \text{on } \theta = 0, \alpha. \tag{2.1}$$

† It also breaks down in an immediate vicinity of the corner, since it implies an (unphysical) pressure singularity  $p = O(r^{-1})$ ; in practice, this means that there is always a small leakage of fluid through a small gap between the planes – an important practical consideration, which is not, however, treated in this paper.

‡ *Note added in proof.* Dr E. Erdogan has drawn our attention to the interesting paper of Inouye (1973) in which the particular case  $\alpha = \frac{1}{2}\pi$  has been studied both by a boundary-layer technique (which seems to be applicable only when  $U > 0$ ) and by the expansion technique advocated here. Inouye obtained the first correction  $\psi_2$ , but he did not attempt to obtain subsequent terms or to establish the radius of convergence of the series.

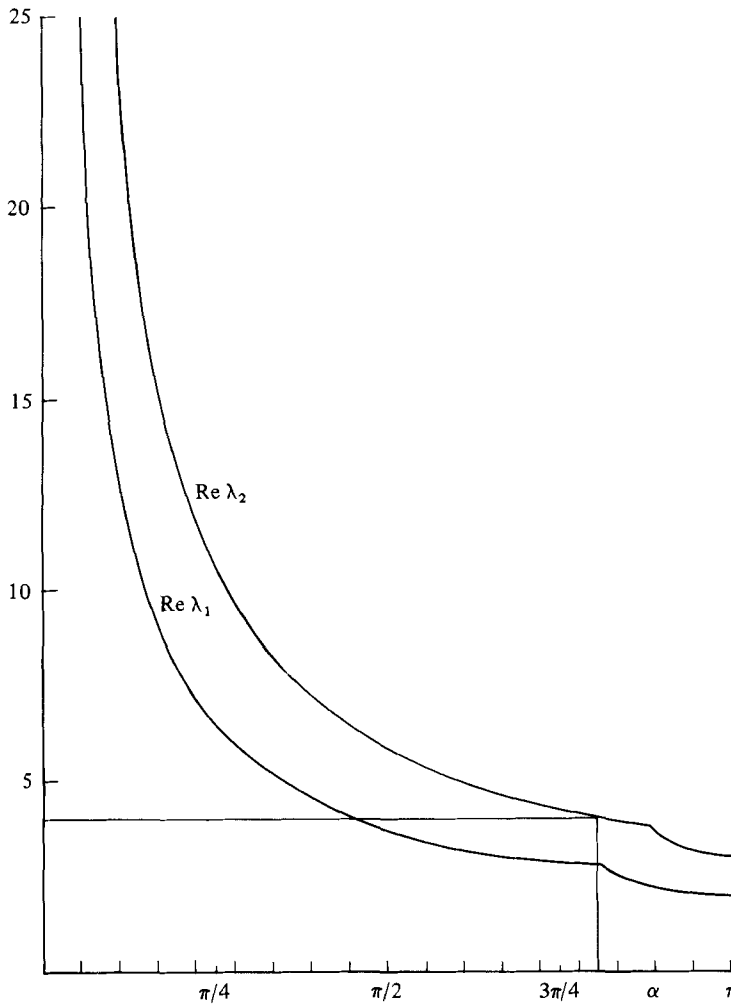


FIGURE 2. Exponents of dominant eigenfunctions as functions of  $\alpha$ ; see the inequalities (2.6) for the Taylor problem and (5.5) for the hinged-plate problem.

This has the well-known form (Moffatt 1964, Lugt & Schwiderski 1965, Weinbaum 1968, Liu & Joseph 1977)

$$\psi_c(r, \theta) = \operatorname{Re} \sum_{n=1}^{\infty} A_n r^{\lambda_n} g_n(\theta), \tag{2.2}$$

where the  $\lambda_n$  are the roots (with positive real part) of

$$\sin(\lambda_n - 1)\alpha = (-1)^n (\lambda_n - 1) \sin \alpha, \tag{2.3}$$

ordered so that

$$0 < \operatorname{Re} \lambda_1 \leq \operatorname{Re} \lambda_2 \leq \dots \tag{2.4}$$

(complex solutions occurring in complex conjugate pairs). The functions  $g_n(\theta)$  are given by

$$g_n(\theta) = \begin{cases} \frac{\cos \lambda_n(\theta - \frac{1}{2}\alpha)}{\cos \frac{1}{2}\lambda_n \alpha} - \frac{\cos(\lambda_n - 2)(\theta - \frac{1}{2}\alpha)}{\cos \frac{1}{2}(\lambda_n - 2)\alpha} & (n \text{ odd}) \\ \frac{\sin \lambda_n(\theta - \frac{1}{2}\alpha)}{\sin \frac{1}{2}\lambda_n \alpha} - \frac{\sin(\lambda_n - 2)(\theta - \frac{1}{2}\alpha)}{\sin \frac{1}{2}(\lambda_n - 2)\alpha} & (n \text{ even}) \end{cases} \tag{2.5}$$

and the (complex) constants  $A_n$  are determined in (in principle) by conditions far from the corner. The apparent freedom here simply reflects the fact that additional ‘conditions at infinity’ must be imposed on  $\psi$  in order to make the solution of the problem (1.3), (1.4) unique, even in the inertia-free limit. It is clear from (2.5) that odd/even values of  $n$  correspond to flows that are antisymmetric/symmetric about  $\theta = \frac{1}{2}\alpha$ . The computed variation of  $\text{Re } \lambda_1$  and  $\text{Re } \lambda_2$  with  $\alpha$  is shown in figure 2.

The solution (2.2) should clearly participate in nonlinear (inertial) interactions, leading to additional terms in the general solution of the problem (1.3), (1.4). However, the dominant behaviour for  $r|U|/\nu \ll 1$  is given by the first  $N$  terms of the expansion (1.6) where

$$N < \text{Re } \lambda_1(\alpha) \leq N + 1, \tag{2.6}$$

subsequent terms being dominated by eigenfunction contributions. For example (from figure 2) when  $\alpha = \frac{1}{2}\pi, \frac{1}{4}\pi, \frac{1}{8}\pi$ , we have  $N = 3, 6, 11$  respectively. For small  $\alpha$ ,  $N$  becomes large, and the solution becomes progressively less sensitive to eigenfunction contributions. For all values of  $\alpha$  in the range  $0 < \alpha < \pi$ , the first inertial correction, given by  $\psi_2$  in (1.6), dominates over any eigenfunction contribution, and may therefore be regarded as having absolute significance, independent of conditions ‘at infinity’. (The limiting case  $\alpha \rightarrow \pi$  is special, in that  $\lambda_1(\pi) = 2$ ; this case will be treated separately below.)

### 3. The first inertial correction $\psi_2(r, \theta)$

With  $n = 2$ , (1.8) becomes

$$\left(\frac{d^2}{d\theta^2} + 4\right) \frac{d^2 f_2}{d\theta^2} = -\left(f_1 \frac{d}{d\theta} + f_1'\right) \left(\frac{d^2}{d\theta^2} + 1\right) f_1 = F_1(\theta), \quad \text{say}, \tag{3.1}$$

where  $f_1$  is given by (1.1). Substitution gives

$$F_1(\theta) = (2BC + C^2 - D^2) \sin 2\theta - 2(B + C) D \cos 2\theta + 4CD \theta \sin 2\theta + 2(C^2 - D^2) \theta \cos 2\theta, \tag{3.2}$$

and the solution of (3.1) satisfying (1.9) (with  $n = 2$ ) may then be found by elementary techniques in the form

$$f_2(\theta) = E\theta \cos 2\theta + F\theta \sin 2\theta + G\theta^2 \cos 2\theta + H\theta^2 \sin 2\theta + P + Q\theta + R \cos 2\theta + S \sin 2\theta, \tag{3.3}$$

where  $E, F, \dots, S$  are constants, depending only on  $\alpha$ , whose values are obtained in the Appendix.

The streamlines  $\psi_1 + \psi_2 = \text{constant}$  (for  $\alpha = \frac{1}{2}\pi$ ) are shown by the dashed curves in figure 1*a* ( $U < 0$ ) and 1*b* ( $U > 0$ ); in the former case, inertia tends to compress the streamlines towards the fixed wall  $\theta = \alpha$ , i.e. we see the beginnings of a wall-jet type of flow on  $\theta = \alpha$ , whereas in the latter case the flow has a sink-like character in the region  $\frac{1}{4}\pi \lesssim \theta \lesssim \frac{1}{2}\pi$ .

The case  $\alpha = \pi$

As noted above, this case needs special treatment, and indeed this is now evident also from the solution (3.3), in which (see appendix) the constants  $P$  and  $R$  become infinite as  $\alpha \rightarrow \pi$ ; in fact, writing  $\alpha = \pi - \epsilon$ , the asymptotic form of (3.3) is

$$f_2(\theta) \sim -\frac{1}{32\epsilon} (1 - \cos 2\theta) - \frac{3\theta(1 - \cos 2\theta)}{32\pi^2} + \frac{(\theta - 2\pi)\theta \sin 2\theta}{16\pi^2} + O(\epsilon). \tag{3.4}$$

The singular behaviour that occurs when  $\epsilon \rightarrow 0$  can be resolved (cf. Moffatt & Duffy 1980) by choosing  $A_1$  (in (2.2)) so that

$$\lim_{\epsilon \rightarrow 0} \left[ \left( \frac{rU}{\nu} \right)^2 f_2(\theta) + A_1 r^\lambda g_1(\theta) \right], = \tilde{\psi}_2 \text{ say,} \tag{3.5}$$

is finite. Now, for  $\epsilon \ll 1$ ,  $\lambda_1 \sim 2(1 + \epsilon/\pi)$  from (2.3), and, from (2.5),

$$g_1(\theta) \sim (\cos \theta - 1) - \frac{2\epsilon\theta}{\pi} \sin 2\theta + O(\epsilon^2). \tag{3.6}$$

Hence we require  $A_1 = -U^2/32\epsilon\nu^2$ , and the appropriate inertial correction when  $\alpha = \pi$  is, from (3.5),

$$\tilde{\psi}_2 = \frac{1}{32\pi^2} \left( \frac{Ur}{\nu} \right)^2 [(2 \ln r - 3\theta)(1 - \cos 2\theta) + 2\theta(\theta - \pi) \sin 2\theta]. \tag{3.7}$$

#### 4. Numerical determination of higher terms in the expansion (1.6)

It is of some interest to investigate the rate of convergence of the expansion (1.6), since this is the ‘driven’ ingredient of the flow which is present irrespective of remote conditions. We have integrated the equations for the particular case  $\alpha = \frac{1}{2}\pi$ , for  $n = 3, 4, \dots, 10$ , using a standard finite-difference procedure†; the number of steps  $N_\theta$  in the  $\theta$  direction was variable, the maximum value used being 280. The partial sums

$$\Psi_N = \sum_1^N \rho^n f_n(\theta) \tag{4.1}$$

are shown in table 1, for  $\theta = \frac{1}{4}\pi$  and for various values of  $\rho = rU/\nu$  and of  $N$ . The results suggest a radius of convergence  $\rho_c$  somewhat less than 10. The streamlines  $\Psi_3 = \text{constant}$  are shown in figure 3, and they are close to the streamlines  $\Psi_2 = \text{constant}$  for  $|\rho| < 5$ , where the convergence appears to be strong.

---

$N \backslash \rho$	5	6	8	10
1	-1.080	-1.296	-1.728	-2.160
2	-1.283	-1.588	-2.247	-2.971
5	-1.397	-1.808	-2.891	-4.506
10	-1.399	-1.809	-2.786	-3.357

---

TABLE 1. Values of  $\psi_N(\rho, \theta = \frac{1}{4}\pi)$ , where  $\rho = rU/\nu$ .

† Full computational details may be found in Hancock (1981).

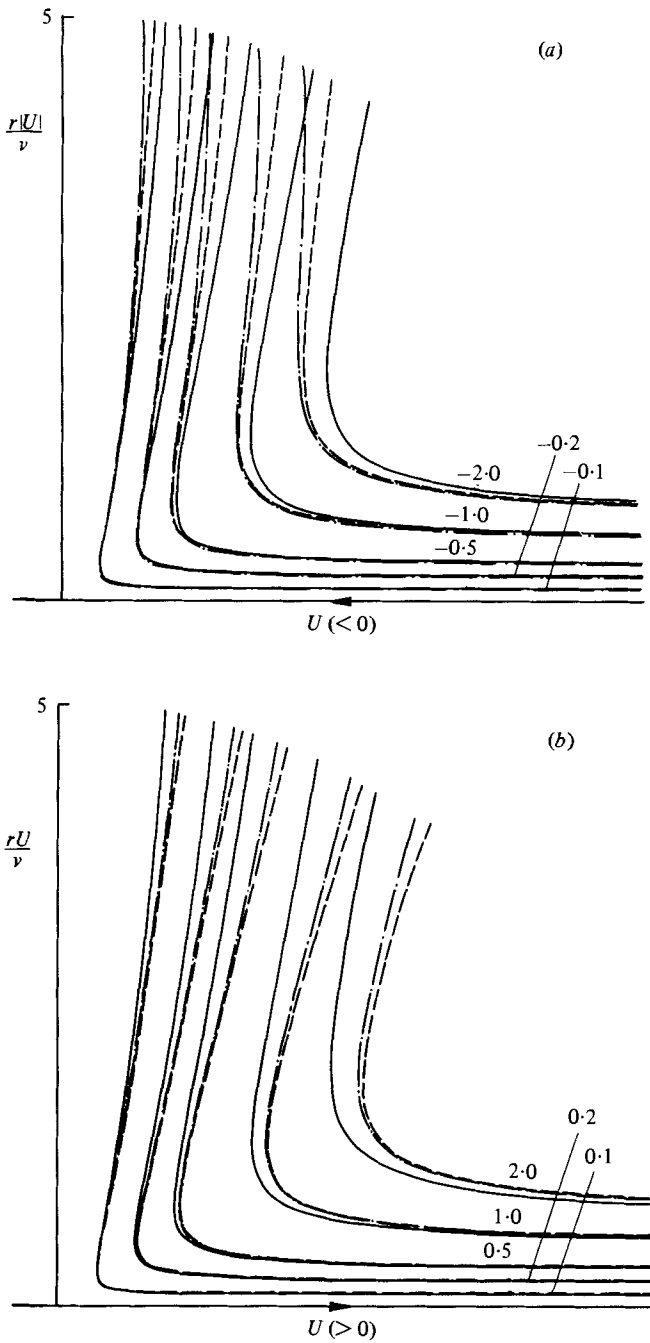


FIGURE 3. Streamlines obtained from the numerical solution for the Taylor problem, with  $\alpha = \frac{1}{2}\pi$ ; —  $\Psi_1$ ; - - -  $\Psi_2$ ; ····  $\Psi_3$  (see (4.1)).

---

$N_\theta$	$a_1$	$a_2$
40	2.14093488	-0.0561335
80	2.14092432	-0.0573850
120	2.14092333	-0.0578547
160	2.14092309	-0.0580994
200	2.14092300	-0.0582494
240	2.14092297	-0.0583508
280	2.14092295	-0.0584238
$\infty$	2.1409229...	-0.0588739

---

TABLE 2. Dependence of the computed coefficients  $a_1$  and  $a_2$  on number of grid points  $N_\theta$ , the values for  $N_\theta = \infty$  being obtained analytically.

---

$n$	$a_n$	$n$	$a_n$
1	+2.1409229 E+00	13	-9.7262179 E-13
2	-5.8873180 E-02	14	+1.4245417 E-13
3	-6.6765159 E-04	15	+2.2946768 E-14
4	+9.7142473 E-05	16	-3.2082762 E-15
5	+5.4877329 E-05	17	-3.2095151 E-16
6	+5.3913679 E-06	18	-1.3783152 E-17
7	-9.7663279 E-07	19	+3.2277461 E-18
8	-1.3054515 E-07	20	+3.2717161 E-19
9	+9.7903752 E-09	21	-2.0344861 E-20
10	+1.7532554 E-09	22	-4.7292192 E-21
11	-2.6119257 E-11	23	-3.7425476 E-23
12	-1.8402067 E-11	24	+5.0058987 E-23
		25	+3.5599210 E-24

---

TABLE 3. Extrapolated values of  $a_n$ .

The wall stress on  $\theta = 0$  is given by

$$\tau = \frac{\nu}{r^2} \left( \frac{\partial^2 \psi}{\partial \theta^2} \right)_{\theta=0} = U^2 \sum_1^{\infty} a_n \rho^{n-2}, \quad (4.2)$$

where  $a_n = f_n''(0)$ . The analytical results of § 3 give, with  $\alpha = \frac{1}{2}\pi$ ,

$$a_1 = \frac{4\pi}{\pi^2 - 4} = 2.1409229\dots, \quad (4.3)$$

$$a_2 = \frac{\pi(4\pi^4 - 8\pi^2 - 352)}{64(\pi^2 - 4)} = -0.0588739\dots, \quad (4.4)$$

and these are compared in table 2 with numerical results for different values of  $N_\theta$ . Using the Aitken  $\delta^2$ -extrapolation procedure, the exact values ( $N_\theta \rightarrow \infty$ ) of each  $a_n$  were estimated from similar sequences. This calculation required less computer storage, and it was possible to find the  $a_n$  for  $n = 3, 4, \dots, 25$ ; these values are shown in table 3.

We are greatly indebted to Professor Milton Van Dyke who has suggested the means by which the singularities of the function  $\sum a_n z^n$  may be located. Firstly, the pattern



$N$	$\rho_c$	$\beta/\pi$
3	5.455	0.3556
4	8.447	0.4153
5	8.654	0.3874
6	8.840	0.4022
7	9.170	0.4119
8	9.092	0.4117
9	9.094	0.4118

TABLE 4. Poles  $z_c = \rho_c e^{\pm i\beta}$  of the  $[N/N]$  Padé approximants for  $N = 1, 2, \dots, 9$ . (For  $N = 10, 11$ , the Padé approximant is degenerate due to the near-coincidence of a zero of the numerator with  $z = z_c$ ; for  $N = 12$ , the pole  $z = z_c$  reappears at  $z_c \approx 9.1e^{\pm 0.41\pi i}$ .)

of signs of the coefficients settles down to  $(+ + - - -)$ . A model function exhibiting a similar pattern is

$$f(z) = -\frac{1}{2} \left( \frac{1}{e^{i\beta} - z} + \frac{1}{e^{-i\beta} - z} \right) = \frac{-\cos \beta + z}{1 - 2z \cos \beta + z^2} = -\sum_{n=0}^{\infty} z^n \cos(n+1)\beta, \quad (4.5)$$

with  $\beta = \frac{2}{3}\pi$ ; this function has simple poles at  $z = e^{\pm i\beta}$ , and this suggests that the series  $\sum a_n z^n$  may have singularities near  $\arg z = \pm \frac{2}{3}\pi$ .

Secondly, the dominant singularities may be located using Padé approximants. Table 4 shows the poles  $z_c = \rho_c e^{\pm i\beta}$  of the  $[N/N]$  Padé approximants for  $N = 3, 4, \dots, 9$  (Van Dyke, private communication). The position rapidly stabilizes to  $z_c \approx 9.1e^{\pm 0.41\pi i}$ ; as expected, the angle  $0.41\pi$  is near to the value  $\frac{2}{3}\pi$  suggested by the pattern of signs. The inference is that the series (4.2) (and so presumably the series (1.6)) has radius of convergence

$$\rho_c \approx 9.1. \quad (4.6)$$

### 5. The hinged-plate problem

Consider now the related problem sketched in figure 4: the plates  $\theta = \pm \frac{1}{2}\alpha$  are hinged at  $O$ , and rotate about  $O$  with angular velocities  $\pm \omega$  (so that  $d\alpha/dt = 2\omega$ ). We suppose for simplicity that  $\omega$  is constant; even so, the resulting flow is necessarily unsteady due to the changing geometry; in the Stokes approximation, however, the stream function  $\psi_s(r, \theta)$  is instantaneously determined, and the similarity solution analogous to (1.1) is (Moffatt 1964)

$$\psi_s = \frac{1}{2}\omega r^2 f_1(\theta, \alpha) = -\frac{1}{2}\omega r^2 \frac{\sin 2\theta - 2\theta \cos \alpha}{\sin \alpha - \alpha \cos \alpha}. \quad (5.1)$$

Figure 4 shows the streamlines  $\psi_s = \text{constant}$  (solid curves) for  $\alpha = \frac{1}{4}\pi$ .

Two simple properties of this stream function are worth noting in the present context.† Firstly, when  $\alpha = \frac{1}{2}\pi$ ,  $\nabla^2 \psi_s = 0$ ; for this particular angle, it might be thought that (5.1) provides an exact (irrotational) solution of the Navier–Stokes equations; however, there is an inertial correction due to unsteadiness (see (5.11) below). Secondly, when  $\sin \alpha = \alpha \cos \alpha$ , i.e. when  $\alpha \approx 257^\circ$ ,  $\psi_s$  is singular because (Moffatt & Duffy 1980)

† As for the Taylor problem, there is a pressure singularity ( $p \sim \ln r$ ) at  $r = 0$ , which we make no attempt to resolve in this paper.

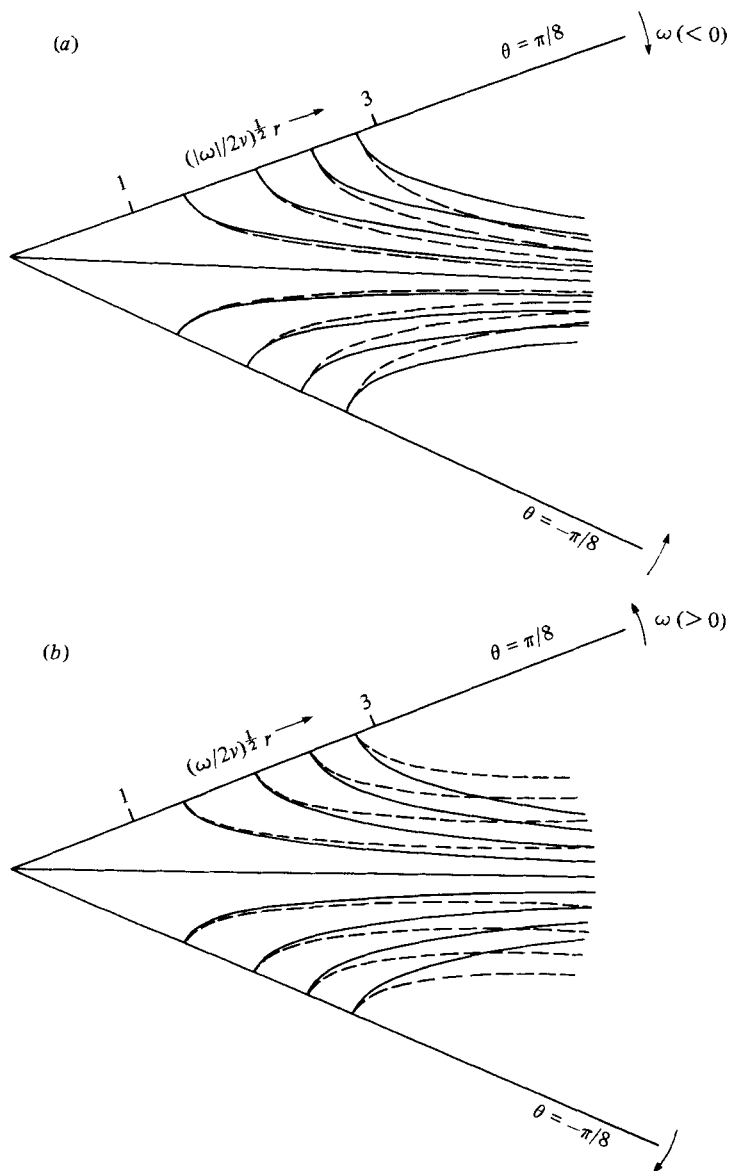


FIGURE 4. The hinged plate problem; streamlines for  $\alpha = \frac{1}{4}\pi$ ; the solid curves are the streamlines for the Stokes flow  $\psi_1$  ( $= \psi_s/\nu = \text{constant}$  (equation (5.1))); the dashed lines include the first-order inertial correction  $\psi_2$ . (a)  $\omega < 0$ ; (b)  $\omega > 0$ .

an eigenfunction solution  $r^\lambda f(\theta)$  with  $\lambda = 2$  exists for this critical value of  $\alpha$ ; the singularity can be resolved only when the eigenfunction solution is included, and this leads to an  $r^2 \ln r$  behaviour. The same problem arises in a more acute form when inertial corrections are considered – see (5.8) below.

For general values of  $\alpha$ , inertia forces associated both with nonlinearity and with unsteadiness are important. We require to find a stream function  $\psi$  satisfying

$$\nu \nabla^4 \psi = -\frac{1}{r} \frac{\partial(\psi, \nabla^2 \psi)}{\partial(r, \theta)} + \frac{\partial}{\partial t} \nabla^2 \psi, \quad (5.2)$$

and subject to the boundary conditions

$$\frac{\partial \psi}{\partial r} = \mp \omega r, \quad \frac{\partial \psi}{\partial \theta} = 0 \quad \text{on} \quad \theta = \pm \frac{1}{2}\alpha(t). \tag{5.3}$$

The series solution analogous to (1.6) has the form

$$\psi = \nu \Sigma \psi_n, \quad \psi_n = \left(\frac{\omega r^2}{2\nu}\right)^n f_n(\theta, \alpha). \tag{5.4}$$

Again, eigenfunction contributions can also intervene in the general solution; here we are concerned only with flows symmetric about  $\theta = 0$  (on the assumption that the remote conditions introduce no asymmetry), i.e. with even values of  $n$  in (2.3); the first  $N$  terms of (5.4) dominate over all eigenfunction contributions where now

$$2N < \text{Re } \lambda_2 \leq 2(N + 1). \tag{5.5}$$

For  $\alpha \gtrsim 145^\circ$ , the inertial correction  $\psi_2$  is always dominated by the eigenfunction  $r^{\lambda_2} g_2(\theta)$ , i.e. for such large angles inertial effects are necessarily associated with the ‘remote’ conditions. For  $\alpha \lesssim 145^\circ$  however, at least the term  $\psi_2$  is always physically significant, and we therefore focus attention on this leading-order inertial effect in what follows.

Substitution of (5.4) into (5.2) leads to a succession of linear equations for the  $f_n(\theta, \alpha)$ : the equation for  $f_2$  (using the expression (5.1) for  $f_1$  and the fact that

$$\partial f_1 / \partial t = 2\omega \partial f_1 / \partial \alpha)$$

reduces to

$$\left(\frac{\partial^2}{\partial \theta^2} + 16\right) \left(\frac{\partial^2}{\partial \theta^2} + 4\right) f_2 = \frac{16(\cos \alpha \sin 2\theta - 2\theta)}{(\sin \alpha - \alpha \cos \alpha)^2}, \tag{5.6}$$

and the solution, subject to the conditions

$$f_2 = \partial f_2 / \partial \theta = 0 \quad \text{on} \quad \theta = \pm \frac{1}{2}\alpha \tag{5.7}$$

is

$$f_2 = \frac{B \sin 2\theta + D \sin 4\theta - 4 \sin^3 \alpha (2\theta \cos 2\theta \cos \alpha - 3\theta)}{24 \sin^3 \alpha (\sin \alpha - \alpha \cos \alpha)^2}, \tag{5.8}$$

where

$$\left. \begin{aligned} B &= \sin 2\alpha (4 + \cos 2\alpha) - \alpha (1 + 8 \cos 2\alpha + \cos^2 2\alpha), \\ D &= 5\alpha \cos \alpha - \sin \alpha (4 + \cos \alpha). \end{aligned} \right\} \tag{5.9}$$

Note that a new singularity appears when  $\alpha = \pi$ ; this singularity can be resolved by including appropriate eigenfunction contributions (as in §3 above), the ultimate result being, for  $\alpha = \pi$ ,

$$\tilde{\psi}_2 = \frac{1}{3\pi^2} \left(\frac{\omega r^2}{2\nu}\right)^2 (1 + \cos 2\theta) \{5 \sin 2\theta \ln r + \theta(5 \cos 2\theta - 4)\}. \tag{5.10}$$

This result is, however, of dubious significance since, as noted above,  $\text{Re } \lambda_2 < 4$  for  $\alpha \gtrsim 145^\circ$ ; in fact, for  $\alpha = \pi$ ,  $\lambda_2 = 3$ , and the corresponding contribution to  $\psi$ , if present, will certainly dominate over (5.10) near  $r = 0$ .

When  $\alpha = \frac{1}{2}\pi$  (in which case  $\nabla^2 \psi_1 = 0$  as remarked above) the inertial correction simplifies to

$$\psi_2 = \frac{1}{8} \left(\frac{\omega r^2}{2\nu}\right)^2 (\pi \sin 2\theta - \sin 4\theta - 4\theta). \tag{5.11}$$

Figure 4 shows the streamlines of  $\psi_1 + \psi_2$  (for  $\alpha = \frac{1}{4}\pi$ ) as dashed curves for  $\omega < 0$  (figure 4*a*) and  $\omega > 0$  (figure 4*b*). In the former case, a jet-type flow tends to develop as the fluid is squeezed out of the gap; in the latter case, inertia forces tend to spread the flow more evenly over the range of  $\theta$  (relative to the Stokes flow).

It would of course be possible to obtain subsequent terms of the series (5.4) numerically (as done above for the Taylor problem). The limited additional information that this would provide, however, makes this an exercise of doubtful value. A more interesting problem might be to allow for unsteadiness in  $\omega$ , and hence for example to study the development of the flow due to angular acceleration of the plates from a state of rest. We leave this problem to a future investigation.

We are grateful to a referee of a previous version of this paper, whose penetrating comments led to significant improvements; to Professor Milton Van Dyke for his suggestions concerning the use of Padé approximants; to Professor S. N. Curle for discussion on the topic of series improvement; and to the Science Research Council for supporting the work of one of us (C. H.) by a Research Studentship.

### Appendix

In equation (3.2), let

$$\left. \begin{aligned} K_1 &= 2BC + C^2 - D^2, & K_2 &= -2(B + C)D, \\ K_3 &= 4CD, & K_4 &= 2(C^2 - D^2), \end{aligned} \right\} \tag{A 1}$$

where  $B, C, D$ , are given by (1.2). A particular integral of (3.1) is then

$$f_2^{(p)} = E\theta \cos 2\theta + F\theta \sin 2\theta + G\theta^2 \cos 2\theta + H\theta^2 \sin 2\theta, \tag{A 2}$$

where, as is easily verified,

$$\left. \begin{aligned} 32E &= 2K_1 - 3K_4, & 32F &= -2K_2 - 3K_3, \\ 16G &= K_3, & 16H &= -K_4. \end{aligned} \right\} \tag{A 3}$$

The complementary function is

$$f_2^{(c)} = P + Q\theta + R \cos 2\theta + S \sin 2\theta, \tag{A 4}$$

and, with  $f_2 = f_2^{(p)} + f_2^{(c)}$ , the boundary conditions (1.9) give

$$\left. \begin{aligned} P + R &= 0, \\ Q + 2S + E &= 0, \\ P + Q\alpha + R \cos 2\alpha + S \sin 2\alpha &= -X(\alpha), \\ Q - 2R \sin 2\alpha + 2S \cos 2\alpha &= -X'(\alpha), \end{aligned} \right\} \tag{A 5}$$

where  $X(\alpha) = E\alpha \cos \alpha + F\alpha \sin \alpha + G\alpha^2 \cos \alpha + H\alpha^2 \sin \alpha$  and  $X'(\alpha)$  is the derivative of  $X$ , regarding  $E, F, G, H$  as constants. Solving (A 5), we find

$$\left. \begin{aligned} P = -R &= \frac{2E\alpha \sin^2 \alpha - 2X(\alpha) \sin^2 \alpha - (E - X'(\alpha)) (\alpha - \sin \alpha \cos \alpha)}{4 \sin \alpha (\sin \alpha - \alpha \cos \alpha)}, \\ Q &= \frac{2X(\alpha) \cos \alpha - X'(\alpha) \sin \alpha - E \sin \alpha}{2(\sin \alpha - \alpha \cos \alpha)}, \\ S &= \frac{(2E\alpha \cos \alpha - 2X(\alpha) \cos \alpha - E \sin \alpha + X'(\alpha) \sin \alpha) \sin^2 \alpha}{4(\sin \alpha - \alpha \cos \alpha)}. \end{aligned} \right\} \quad (\text{A } 6)$$

Hence  $f_2(\theta, \alpha)$  is completely determined.

For the particular case  $\alpha = \frac{1}{2}\pi$ , the constants  $E, F, \dots, R, S$  take the values

$$\begin{bmatrix} E \\ F \\ G \\ H \\ P \\ Q \\ R \\ S \end{bmatrix} = \frac{1}{64(\pi^2 - 4)^2} \begin{bmatrix} -8(\pi^2 + 12) \\ -16\pi(\pi^2 + 6) \\ 64\pi \\ 16(\pi^2 - 4) \\ \pi(\pi^4 + 14\pi^2 - 24) \\ -4\pi^2(\pi^2 + 8) \\ -\pi(\pi^4 + 14\pi^2 - 24) \\ 2(\pi^2 + 6)(\pi^2 + 4) \end{bmatrix} \quad (\text{A } 7)$$

The streamline plots in figure 1 are based on this solution.

REFERENCES

HANCOCK, C. 1981 Corner Flows. Ph.D. thesis, University of Bristol.  
 INOUE, K. 1973 Écoulement d'un fluide visqueux dans un angle droit. *J. de Mécanique* **12**, 609-628.  
 LIU, C. H. & JOSEPH, D. D. 1977 Stokes flow in wedge-shaped trenches. *J. Fluid Mech.* **80**, 443-463.  
 LUGT, H. J. & SCHWIDERSKI, E. W. 1965 Flows around dihedral angles. I. Eigenmotion analysis. *Proc. Roy. Soc. A* **285**, 382-412.  
 MOFFATT, H. K. 1964 Viscous and resistive eddies near a sharp corner. *J. Fluid Mech.* **18**, 1-18.  
 MOFFATT, H. K. & DUFFY, B. R. 1980 On local similarity solutions and their limitations. *J. Fluid Mech.* **96**, 299-313.  
 TAYLOR, G. I. 1960 Similarity solutions of hydrodynamic problems. Article in *Aeronautics and Astronautics (Durand Anniv. Vol.)*, pp. 21-8. Pergamon.  
 TAYLOR, G. I. 1962 On scraping viscous fluid from a plane surface. In *The Scientific Papers of Sir Geoffrey Ingram Taylor*, vol. iv (ed. G. K. Batchelor), pp. 410-413. Cambridge University Press, 1971.  
 WEINBAUM, S. 1968 On the singular points in the laminar two-dimensional near wake flow field. *J. Fluid Mech.* **33**, 39-63.